Egypt. J. Chem. **Vol. 64,** No. 12 pp. 7551 - 7564 (2021)

Egyptian Journal of Chemistry

http://ejchem.journals.ekb.eg/

Preparation and Characterization of A New Family Of Bio-Interpenetrating Network Hydrogel Based On A Green Method

Alaa I.E. Abdelaziz[a*], S.M .Elsaeed[a], E.G. Zaki[a], M.M. Abouly[b], M.E.S. Abdel-Raouf[a], A.M .Al-Sabagh[a]

[a] *Egyptian Petroleum Research Institute, 1 Ahmed El-Zomer Street, Nasr City, 11727, Cairo, Egypt.*
[b] *Chemistry Department, Faculty of Science, Ain Shams University, Cairo, Egypt.*

Abstract

In this work, semi-interpenetrating polymer network hydrogels with and without castor oil (S-2IPNC, S-3IPNC, S-4IPNC, S-2IPN, S-3IPN and S-4IPN) are synthesized using a free-radical solution polymerization in presence of acrylic acid as a pH-responsive monomer and dimethyl aminoethyl methacrylate as a thermoresponsive monomer with carboxymethyl cellulose (CMC) as a cellulose derivative, potassium persulphate and N, N'-methylene bisacrylamide. Castor oil, as a green chemical material, is incorporated with a ratio (1:2) to CMC. The semi-interpenetrating network structures are formed and justifications are done by ATR-FTIR and Raman spectroscopy to assure their chemical composition. TGA, SEM, XRD and AFM approve thermogravimetric analysis, phase morphology, crystallinity and surface topography, respectively. The results show that the addition of castor oil enhances the texture and stability of hydrogels. It is concluded that S-IPNC hydrogels show higher swelling capacity than S-IPN hydrogels at lower NaCl concentration and pH range (5-7), due to increasing the osmotic pressure.Therefore, castor oil could be used as a green material in interpenetrating network hydrogels for water-saving applications.According to the principle of sustainable growth, environmentally biopolymer hydrogels pose a significant potential for using as water storage in the agricultural sector.

Keywords: AFM; Castor oil; Dimethyl aminoethyl; Interpenetrating polymer network (IPN); Swelling behavior; Thermal analysis.

1. Introduction

The principles of green chemistry are widely spreading through industrial processes. The main reason for using green chemistry is to reduce problems related to human health and environmental risks by replacement of petroleum-based materials with natural polymer materials involved in different applications[1-3].The hydrogel is known as a network formed of crosslinked polymers that can hold the absorbed water within its pores due to the presence of hydrophilic groups, such as carboxyl and hydroxyl groups, in their polymer chains[4, 5]. A distinct group is that of macromolecular hydrogels, composed of superabsorbent hydrogels that can absorb huge quantities of water and retain it [6, 7]. They show biodegradability, high swelling rate (SR), excellent water retention ratio (WRR) and high swelling capacity [8, 9], which endows them to have widespread practical applications such as hygienic products[10],agriculture[11],wastewater treatment [12, 13], printing applications[14], drug delivery[15, 16], tissue engineering[17, 18], sensor and actuator [19-21] and solar cells [22-26].

IPNs (interpenetrated polymer networks) are three-dimensional polymer networks that combine two polymers at least one of them is cross-linked or synthesized in the network form using various functional groups that have high water-swelling properties.

IPNs are better than hydrogels as they have different characteristics that enhance the swelling capacity, mechanical properties and are stable in a wide pH range and at high temperatures [27].

Thermoresponsive hydrogels exhibit a phase separation and volume change above a definite temperature.

There are two main types of thermoresponsive polymers; the first is a lower critical solution temperature (LCST) and the second is upper critical solution temperature (UCST). LCST and UCST are

* Corresponding author e-mail: alaa.abdelaziz89@yahoo.com
Receive Date: 13 June 2021, Revise Date: 14 August 2021, Accept Date: 16 August 2021
DOI: 10.21608/EJCHEM.2021.78987.3991

the critical temperature points where polymer and solvent become miscible below and above it respectively. These hydrogels shrink upon heating above LCST as they become insoluble and more hydrophobic and that leads to gel formation and soluble below LCST. On the contrary, hydrogels have positive temperature-sensitive shrink upon cooling below the UCST and swell above it [28].

Poly(N-isopropylacrylamide) (PNIPAM) and poly(dimethyl aminoethyl methacrylate) (PDMAEMA) resemble the most important temperature-responsive polymers, as the LCST of PNIPAM is 32 ^{o}C [29] while that for PDMAEMA is around 14-50 ^{o}C [30].

Carboxymethylcellulose (CMC) is a cellulose derivative and considers as an essential polymer in different industrial applications. CMC, among all the polysaccharides, is very cheap and easily abundant [31]. Vegetable oils are bio-renewable resources extracted from different plants such as palm oil, soybean oil and castor oil.

Castor oil is a renewable and cost-competitive environmental resource, it also has good flexibility and elasticity due to the presence of a long fatty acid chain, and it leads itself as a thermosetting type material due to its trifunctional nature. It also has a unique structure, with about 90% of the fatty acid chains being ricinoleic acid, which bears a hydroxyl group, making it a useful vegetable oil in the industrial field. As a result of the hydroxyl groups and carbon-carbon double bonds, it is useful in a variety of chemical processes[32, 33]. Moreover, castor oil, among all vegetable oils, is considered as one of the most plentifully and naturally occurring oils, which can be used for the improvement of the polymers with tremendous properties that can be used for numerous applications like lubricants, coating, etc. [34]. Polyols based on vegetable oils, as widely plentiful raw materials, have found many essential applications [11]. For example, polyols based on castor oil are considered environment-friendly and reasonable in cost [35, 36]. Adding castor oil to CMC aims to provide a novel technique to enhance the interfacial adhesion and improve polymer network connectivity

IPNs prepared using castor oil showed enhanced mechanical properties, electrical properties and thermal stability due to high crosslinking density and high content of hydroxyl in castor oil in comparison with other vegetable oils [37, 38]. So, IPNs from castor oil have been developed for different industrial applications [39]. In contrast with different vegetable oils, castor oil can be stored for a long time and stay usable. Castor oil, as a renewable source, can be utilized as a starting material in the synthesis of bio-based polymers to be industrialized and used for upcoming applications [40].

The aim of this work concentrates on three objects, the first one is to synthesize a new family of bio-interpenetrating network hydrogels of DMAEMA monomer with acrylate monomer (AA) using a redox initiator as potassium persulfate (KPS) and a crosslinking agent as N, N′-methylene bisacrylamide (MBA), based on green chemicals such as carboxymethyl cellulose (CMC) and castor oil. The second object is confirmation their chemical structures using ATR-FTIR, Raman spectroscopy, TGA, SEM, XRD and AFM. The third objective is the incorporation of castor oil in IPNs and investigating their swelling properties under different conditions, studying their re-ability for swelling-deswelling, so we could predict their use in environmental/agriculture applications.

2. **Materials and methods**

2.1. Materials

Acrylic acid (AA, analytical grade, Fluka, Germany). dimethyl aminoethyl methacrylate (DMAEMA, analytical grade, Sigma-Aldrich).

Carboxymethylcellulose (CMC, National Company). N,N′-methylene bisacrylamide (MBA, ACROS organic). sodium chloride (NaCl) and potassium persulphate (KPS) were purchased from ADWICK ”commercial”. sodium hydroxide (NaOH , Fisher Chemical Scientific Lab). Castor oil was purchased from the local market and found to contain hydroxyl value 160-162 mg KOH/g, corresponding to 2.7 hydroxyl groups per mole of castor oil. All reagents were used without further purification. Deionized water was used throughout the work.

2.2. Preparation of CMC/Poly(AA-DMAEMA) semi-interpenetrating polymer network with castor oil (S-IPNC) and without castor oil (S-IPN)

This work introduces preparation of a new simultaneous interpenetrating polymer network where acrylate monomer AA and DMAEMA monomer were in situ polymerize, in presence of CMC and castor oil, along with initiator, one is crosslinked by MBA to form a polymer network while the other monomer forms a linear polymer which entrapped into the matrix to form finally a semi IPN.

The desired amount of reactants were placed in a 250 ml flask (four-necked) with a condenser, magnetic

stirrer and a thermometer equipped with a nitrogen line. The superabsorbent hydrogels were synthesized using a free-radical polymerization [41]. In the case of IPNC, CMC and castor oil (2:1) were dispersed into 100 ml of distilled water by constantly stirring for 2 hrs at 60 ° C. About 0.074 g of KPS was added into this dispersion and the mixture was stirred for 10 min at 60 °C to generate radicals, after that, desired ratios of DMAEMA were added in accordance with neutralized Acrylic acid (AA) to the CMC solution then cooling to 40 °C and finally 0.074 gm of MBA was added to terminate the reaction.

To complete the polymerization reaction, the temperature was rose gradually to be at 70 °C and kept for 3hrs.

Then, the samples were immersed in distilled water to remove any unreacted components. Then the samples were put in the oven at 50-60 °C till constant weight.

Conversely, in the case of IPN, castor oil was removed and the same pre-mentioned steps were repeated. The codes and constitutions of the prepared hydrogels are given in Table 1(supplementary file).

2.3. Characterization techniques

Attenuated total reflection-Fourier transform infrared spectroscopy

The chemical structures were confirmed using an attenuated total reflection-Fourier transform infrared spectrophotometer (ATR-FTIR, Bruker Optik Gmbh Ettlingen, Germany), in the range of 4000–400 cm^{-1}, LUMO fully motorized stand-alone FTIR microscope in ATR mode.

Raman spectroscopy

The Raman spectra were recorded with (Dispersive Raman Microscope, Bruker, Senterra) in the spectral range from 45-4500 cm^{-1}. Excitation was done with a 785 nm laser source.

Thermogravimetric analysis

The decomposition profile of samples was thermogravimetrically analyzed using TGA 55 (Meslo, USA). Film samples were placed in a pan of platinum and heated in the range of 30 °C - 600 °C under N_2 atmosphere at a heating rate of 10 °C per minute and weight loss was plotted versus temperature.

Surface morphology techniques

(a) Scanning electron microscopy

Scanning electron microscope (SEM) was used for surface imaging using Quanta FEG 250 (FEI company, USA) available at Egyptian Desalination Research Center of Excellence (EDRC), Desert Research Center (DRC) in Egypt. Samples were mounted onto SEM stubs with 10.1 mm as a distance of work and the voltage of excitation was 20 kV with an in-lens detector.

(b) Atomic force microscope

The surface morphology of prepared hydrogel was investigated using an atomic force microscope (AFM, Flexaxiom Nanosurf, Switzerland).0.1g of the sample was crushed into a fine powder then placed onto a sample holder. The samples were scanned by contact mode. The image size was 10 µm with a constant force 20 nN in air environment with a temperature 20–25 °C.

X-ray diffraction

X-ray diffraction (XRD) patterns of samples was recorded using a PANalytical diffractometer (Siemens, AXSD5005) available at Egyptian petroleum research institute (EPRI) with Cu-Ka radiation (k = 1.54 Å) generated at 40 kV and 40mA in the differential angle (2θ) range of 4-80.

2.4. Measurements of water absorption and swelling properties

The teabag method was used to perform swelling experiments. In this regard, an accurate weight of the powdered hydrogel (0.05 ± 0.01 g) was put in a tea bag and immersed into distilled water at room temperature (25 °C) for 4hrs. Then, the teabag was removed and excess water was allowed to drain. The teabag was removed and allowed to remove excess water. Each sample was repeated at least 3 times, with a maximum error bar ±0.5.

The relation between swollen hydrogel weights and time was recorded every 30 min. Qmax (g g^{-1}) represents water absorption of the hydrogels, it was measured from the change in weight before and after absorption using the following equation (2.1) [7]:

$$\boldsymbol{Qmax} = \frac{\textbf{weight of sample after absorption}}{\textbf{weight of sample before absorption}} \quad \textbf{(2.1)}$$

The absorbance of swollen water for the prepared hydrogels was verified under various conditions as follows.

2.4.1. Swelling of prepared hydrogels at different temperatures

The swelling of prepared hydrogels was monitored at different temperatures (25 °C, 35°C and 45 °C). The bags were removed from distilled water and then weighed. Then, Qmax with temperature was studied.

2.4.2. Swelling of prepared hydrogels at different salt concentrations

The swelling of hydrogel samples was done at different concentrations of NaCl saline solutions (0.2 M, 0.6 M and 1 M) at ambient temperature.

Then Qmax was studied versus salt concentration.

2.4.3. Swelling of prepared hydrogels at different pH

The prepared hydrogels were immersed in distilled water with various pH values (5, 7 and 9) at room temperature. The pH was adjusted using diluting aqueous NaOH (pH 13.0) and HCl (pH 1.0). Then, Qmax with pH was studied.

3. Results and Discussion

3.1. Synthesis of semi- interpenetrating polymer network preparation (in the presence of castor Oil) [S-IPNC]

The superabsorbent hydrogels were synthesized using a free-radical polymerization, by various steps like initiation, propagation and termination of acrylate monomer (AA) and DMAEMA on carboxymethyl cellulose (CMC) and castor oil in the presence of crosslinking agents (MBA). The polymerization reaction was first initiated by potassium persulfate (KPS), which acts as a redox initiator.

The steps of S-IPNC formation are shown in scheme (1) (supplementary file).

The reaction is initiated by anion-radical generation through thermal decomposition of KPS. The –OH and -CH_2 groups are the active sites for grafting to occur. Hydrogen was extracted from –OH groups present in CMC and castor oil using free sulfate anion radicals, leading to the formation of active alkoxy radicals [42]. Then AA and DMAEMA monomers were grafted onto CMC and castor oil backbones that containing radical active sites, leading to the propagation of new polymer chains. Through propagation, pendant –CH=CH_2 of MBA reacts with polymeric chain and so a crosslinked network structure (S-IPNC) is formed [43, 44]. Hence, a mixture of crosslinked (CMC/AA) IPNC and uncrosslinked PDMAEMA chains are formed as PDMAEMA chains were interpenetrated through S-IPNC.

3.2.Structural characterization of S-IPN samples using ATR-FT-IR and Raman spectroscopy

We have thought that vibrational spectroscopy is a powerful tool to explore molecular Interactions between a solvent molecule and a target functional group incorporated into a polymer chain.

The spectra are fundamentally described by aliphatic and polysaccharide groups. The ATR-FTIR spectra of the prepared polymer networks are shown in Fig. (1).

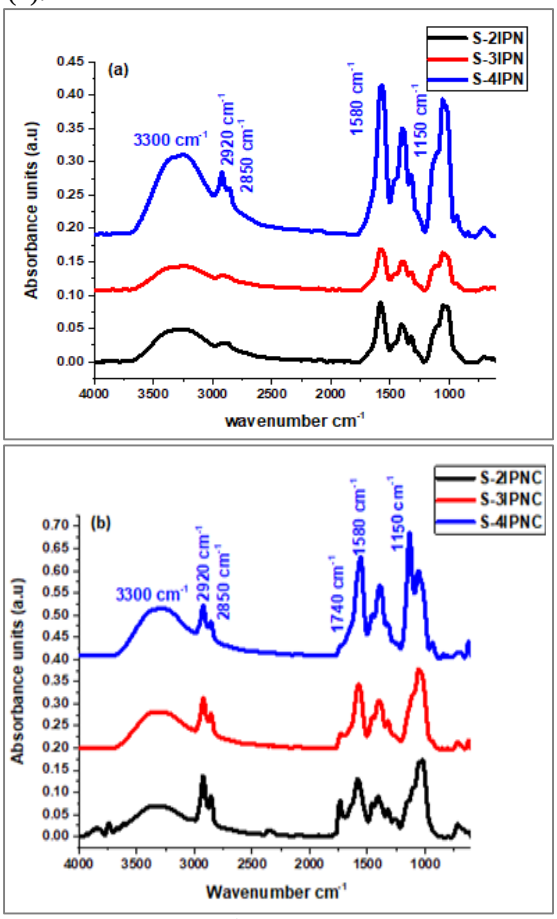

Fig. (1): ATR- FTIR of **(a)** Semi-interpenetrating polymer networks **(S-2IPN) ,(S-3IPN) and (S-4IPN)** with a ratio of acrylic acid (AA) to dimethyl aminoethyl methacrylate (DMAEMA) (1:2) , (1:3) and (1:4) respectively, **(b)** Semi-interpenetrating polymer networks **(S-2IPNC) ,(S-3IPNC) and (S-4IPNC)** with a ratio of acrylic acid (AA) to dimethyl aminoethyl methacrylate (DMAEMA) (1:2) , (1:3) and (1:4) respectively and ratio of castor oil to carboxymethyl cellulose (CMC) (1:2) .

A broad band shows up at 3400–3300 cm^{-1}, related to the O-H stretching. Sharp and intense groups appear at 2920 cm^{-1} and 2850 cm^{-1}, attributed to asymmetric and symmetric C-H stretching for -CH_3 and -CH_2 separately. Amide I band appears around 1700 cm^{-1} due to amidic C=O stretching. Water acts as a proton donor to the C=O group. The band at 1605 (1595) cm^{-1} is characteristic of the aqueous solution and assignable to dihydrogen-bonded C=O groups with water molecules weakened by the steric hindrance of the polymer chains [45]. Another remarkable peak is 1580 cm^{-1}, related to the asymmetric stretching of carboxylate groups (COO-), which means that some of the COO- groups of the polymer are not included in the crosslinking reaction. The ATR-FTIR results showed shifts in the carboxylic and amide groups, indicating the presence of hydrogen bondings within the IPN formation.

Another remarkable band occurs in the spectra around 1315 cm^{-1}, attributed to out-of-plane C-H bending (methylene twisting/wagging) in aliphatic chains. In all ATR spectra, a band shown at 1150 cm^{-1} because of the glycoside C-O-C extending of polysaccharides and a characteristic peak shows up at around 1050 cm^{-1} due to -$N(CH_3)_2$ group in DMAEMA. It is evident that the same peaks increase with increasing the concentration of the monomer.

Raman spectra of prepared polymer networks are shown in Fig.2. With Careful investigation of the provided spectra, one can see that the main difference appears in the spectrum of S-4IPNC, where the ratio of DMAEMA is double-fold than the amount present in S-2IPNC.

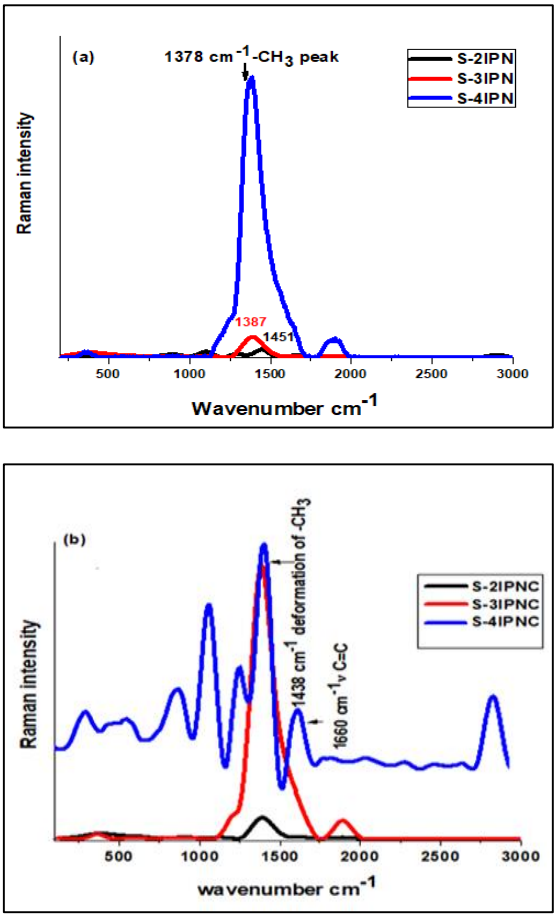

Fig. (2): Raman spectroscopy of **(a)** Semi-interpenetrating polymer networks **(S-2IPN) ,(S-3IPN) and (S-4IPN)** with a ratio of acrylic acid (AA) to dimethyl aminoethyl methacrylate (DMAEMA) (1:2) , (1:3) and (1:4) respectively, **(b)** Semi-interpenetrating polymer networks **(S-2IPNC) ,(S-3IPNC) and (S-4IPNC)** with a ratio of acrylic acid (AA) to dimethyl aminoethyl methacrylate (DMAEMA) (1:2) , (1:3) and (1:4) respectively and ratio of castor oil to carboxymethyl cellulose (CMC) (1:2) .

This sharp peak in the region 1300-1500 cm^{-1} is due to the methyl group. The high intensity of the peak is proportional to the increased number of methyl groups in the molecule, which subsequently increases by increasing DMAEMA concentration. Our finding runs parallel to Roy et al., who observed a near to linear increase of the weight ratio with time and monomer conversion for both monomer concentrations, suggesting that the weight ratio could be predicted depending on the monomer concentration [46]. The low-wavenumber component arises from the hydrogen bond between molecules. In contrast, the high-wavenumber component is due to a non-hydrogen bonded monomer because of the formation of the intermolecular C=O---H-N hydrogen bond in the liquid [47].

For S-2IPNC as an example, the -CH_3 peak appears at 310 cm^{-1} while peaks at 464 cm^{-1} and 567 cm^{-1} are related to symmetric and anti-symmetric $N(CH_3)_2$, respectively. The band of -CH_2 rocking appears at 888 cm^{-1} while for -CH wagging and rocking motions show at 1091 cm^{-1}.The peak appears at 1286 cm^{-1} is assigned to a mixed-mode consisting of the C-N stretching and the C-C stretching modes.

In the region 1400-1700 cm^{-1}.One notices a significant shift for the symmetrical mode of deformation CH_3 to be at 1438 cm^{-1} [48]. The C=C vinyl stretching mode is usually found in the area of 1660-1610 cm^{-1}[49]. Unfortunately, the high Rayleigh diffusion, which arises from heterogeneity dielectric, prevents analysis of the area below 200 cm^{-1}. Hydration leads to shifting in wavenumber, especially the elongation mode C = O, very sensitive to hydrogen bond formation O…X: the formation of hydrogen bond elongates and then weakens the C=O bond, referring to the literature [45, 47, 49].

3.3. Thermogravimetric analysis

Fig.3 illustrates the thermal properties of the prepared polymer networks. The data reveal that the thermal degradation for all the prepared hydrogel started above 200 ºC. The data for weight loss as obtained by the TGA are shown in Table 2.

Almost S-IPN and S-IPNC samples show thermal stability up to 200 ºC, about 20% weight loss occurs in the range 200 ºC - 250 ºC due to the dehydration of molecules and the removal of volatile and/or smaller groups of materials [34]. 70% weight loss for all samples occurs up to 400 ºC due to the decomposition of DMAEMA moieties. Hence, thermogravimetric analysis showed that a higher concentration of castor oil improved the thermal resistance as the hydrogel, which have castor oil in their backbone, is more stable than its counterparts.

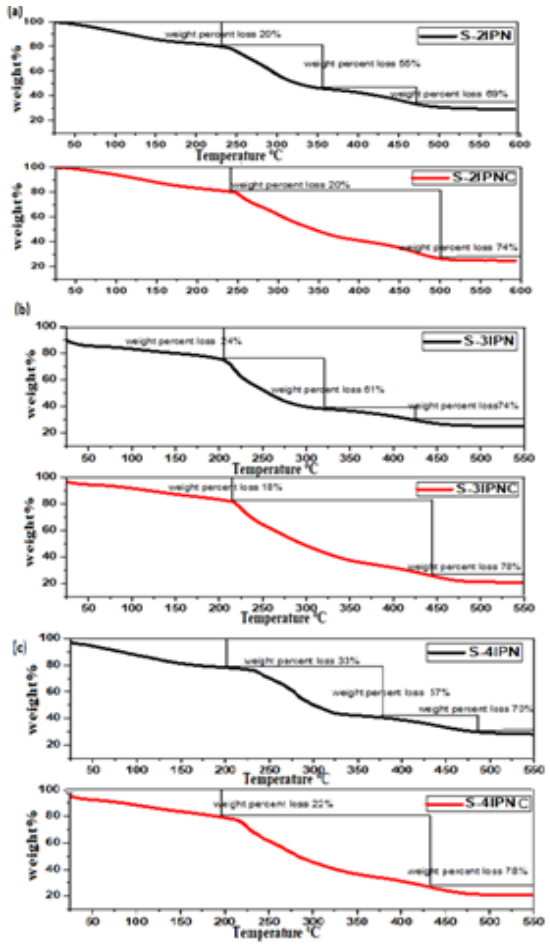

Fig. (3): TGA of the prepared hydrogels **(a)**: Semi-interpenetrating polymer networks **(S-2IPN)** and **(S-2IPNC)** with a ratio of acrylic acid (AA) to dimethyl aminoethyl methacrylate (DMAEMA) (1:2) and castor oil to carboxymethyl cellulose (CMC) (1:2) in case of S-2IPNC, **(b):**Semi- interpenetrating polymer networks **(S-3IPN)** and **(S-3IPNC)** with a ratio of acrylic acid (AA) to dimethyl aminoethyl methacrylate (DMAEMA) (1:3) and castor oil to carboxymethyl cellulose (CMC) (1:2) in case of S-3IPNC and **(c)** Semi-interpenetrating polymer networks **(S-4IPN)** and **(S-4IPNC)** with a ratio of acrylic acid (AA) to dimethyl aminoethyl methacrylate (DMAEMA) (1:4) and castor oil to carboxymethyl cellulose (CMC) (1:2) in case of S-4IPNC.

3.4. Phase morphology using a scanning electron microscope

The morphology of S-3IPN is shown in fig. (4 and 4b) and S-3IPNC samples are shown in 4c, 4d,4e, 4f before and after swelling respectively, at different microscales at (100 µm and 50 µm). SEM images of S-3IPN showed that interconnection pores appear due to the incorporation of CMC into the polymer matrix using interfacial adhesion force that enhances the reinforcement effect. Also, the morphology of S-3IPNC shows the formation of a strong network formed by hydroxyl groups in CMC and castor oil, which forms a hydrogen bond with PDMAEMA and/or AA. After swelling, the absorption process fills up the pores that can be observed from SEM images 4c,4d,4e,4f where pores are filled up and surface morphology is now smooth after absorption. Furthermore, SEM images show a regular distribution of pores with size variation and approved that the interpenetrating polymer network was formed effectively.

Table (2): TGA data corresponding to fig. (3).

Sample Name	Temperature (ºC)/Wt. loss%	Temperature (ºC) /Wt. loss%	Temperature (ºC) /Wt. loss%
S-2IPN	230 ºC/ 20%	360 ºC /55%	497 ºC / 69%
S-2IPNC	242 ºC/ 20%	510 ºC/ 74%	_____
S-3IPN	199 ºC / 24%	308ºC/ 61%	460 ºC / 74%
S-3IPNC	213 ºC / 18%	483 ºC / 78%	_____
S-4IPN	225 ºC / 33%	335 ºC /57%	479 ºC / 70%
S-4IPNC	210 ºC/ 22%	469 ºC / 78%	_____

3.5. Atomic force microscope:

The surface topography of the prepared polymer networks in the 3D image is illustrated in Fig. (5a) and (5b), respectively. All samples showed a granular morphology that characterizes crosslinked CMC/Poly (AA-DMAEMA) polymer network, which is stabilized by hydrogen bonds formed between polar groups of CMC and functional groups of PDMAEMA and/or AA that confirmed with ATR-FTIR studies. The porous structure of the interpenetrating polymer network is very pronounced, as confirmed before using SEM. Fig. (5a) exhibited a coarse morphology with an irregular interconnected granular feature, which became polished after adding castor oil, as shown in Fig. (5b). Moreover, there is an obvious amorphous structure with more uniform crosslinking between polymeric chains. The incorporation of castor oil increases the spacing between chains and diminishes the porosity. The presence of visible pores approves the superabsorbent feature of samples [50] while fig.(5c,5d) show the swelling state of S-3IPN,S-3IPNC respectively as S-3IPNC shows a fully swollen structure with high water uptake as pores

were shown to be filled with water molecules and eventually pores dimensions increase, unlike S-3IPN which shows a partially swollen network. While fig. (5e, 5f) show the de-swelling state of S-3IPN, S-3IPNC respectively as 3IPNC shows a steady network structure, holding water molecules into their pores despite 3IPN which shows a rapid water release that leads to deformation in the topography of 3D polymer network and increasing the size of cavities into a network structure.

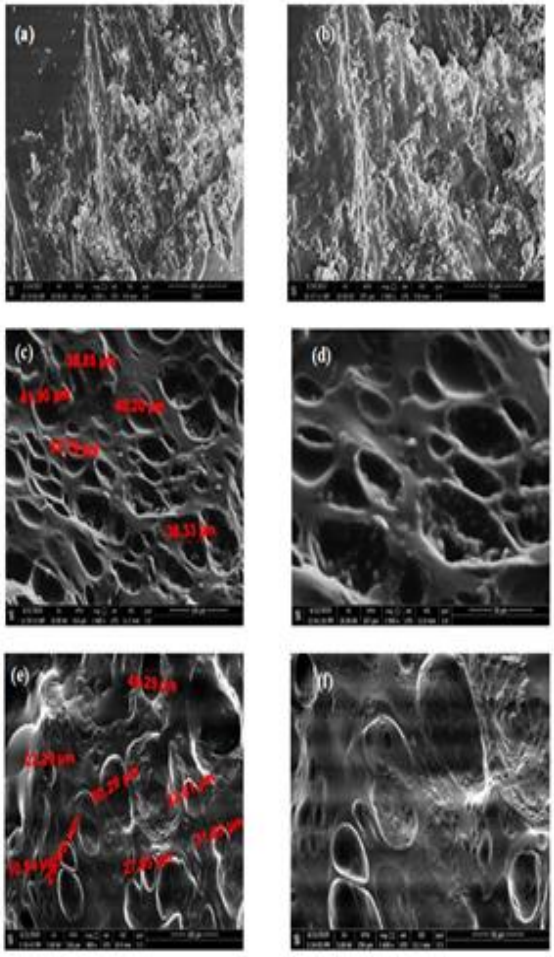

Fig. (4): SEM of **(a,b)** Semi-interpenetrating polymer networks **(S-3IPN)** with a ratio of acrylic acid (AA) to dimethyl aminoethyl methacrylate (DMAEMA) (1:3) at 100µm and 50µm respectively and **(c,d)** Semi-Interpenetrating polymer network **(S-3IPNC)** with a ratio of acrylic acid (AA) to dimethyl aminoethyl methacrylate (DMAEMA) (1:3) and ratio of castor oil to carboxymethyl cellulose (CMC) (1:2) at 100µm and 50µm respectively and **(e,f)** swelling state of **(S-3IPNC)** at 100µm and 50µm respectively.

AFM figures coincide with TGA and cycles of swelling-deswelling of IPN samples and confirm the importance of castor oil in IPN hydrogels which is considered as a promising green component that achieves a pioneering role in enhancing a network structure with a constant arrangement and high internal stability

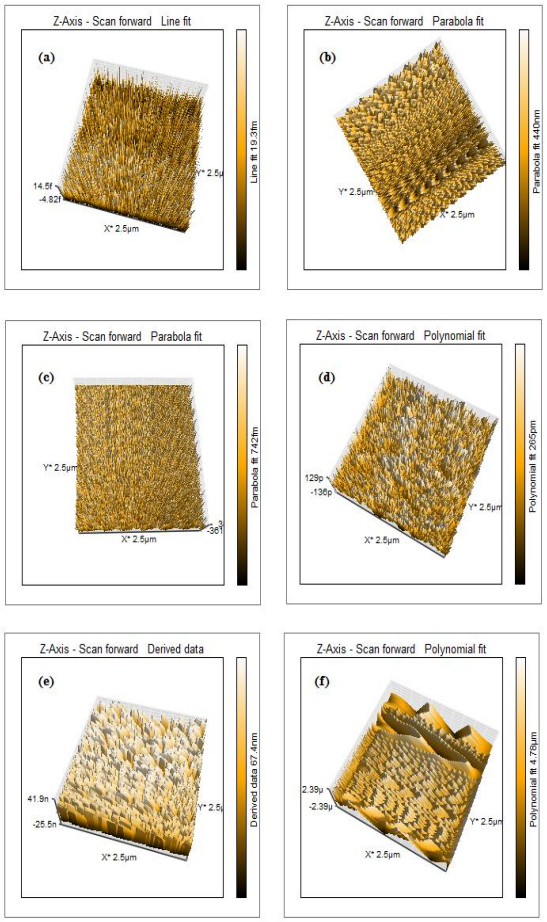

Fig. (5): AFM of **(a)** Semi-interpenetrating polymer networks **(S-3IPN)** with a ratio of acrylic acid (AA) to dimethyl aminoethyl methacrylate (DMAEMA) (1:3) and **(b)** Semi- Interpenetrating polymer network **(S-3IPNC)** with a ratio of acrylic acid (AA) to dimethyl aminoethyl methacrylate (DMAEMA) (1:3) and ratio of castor oil to carboxymethyl cellulose (CMC) (1:2) at 2.5 µm respectively, **(c, d)** swelling state of **(S-3IPN)** and **(S-3IPNC)** at 2.5 µm respectively and **(e,f)** de-swelling state of **(S-3IPN)** and **(S-3IPNC)** at 2.5 µm respectively.

3.6. X-ray Diffraction:

X-ray diffraction (XRD) is commonly used to determine whether the materials are crystalline or amorphous. Intense and sharp peaks in the diffraction pattern of a sample are characteristic of crystalline materials, while amorphous materials show no intense peaks. XRD patterns of S-2IPN, S-2IPNC, S-3IPN, S-3IPNC, S-4IPN, and S-4IPNC samples are shown in Fig. (6) indicate having amorphous properties due to low intense peaks and wide halos. The patterns of S-3IPN and S-3IPNC show peaks between 2Θ values of 28-59 ^{0,} which indicate grafting of poly (DMAEMA) on CMC. That shows the enhancement of crystallinity in the superabsorbent composite.

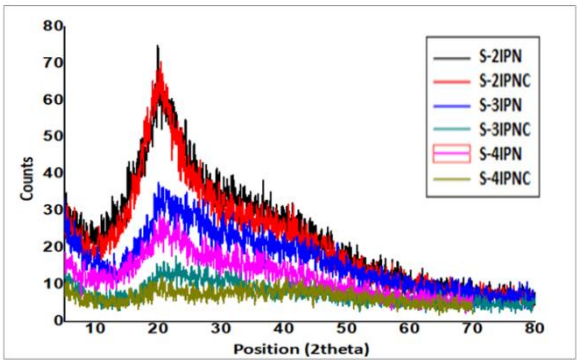

Fig. (6): XRD of Semi-interpenetrating polymer networks**(S-2IPN)** ,**(S-2IPNC)** with a ratio of acrylic acid (AA) to dimethyl aminoethyl methacrylate (DMAEMA) (1:2) , **(S-3IPN)** , **(S-3IPNC)** with a ratio of acrylic acid (AA) to dimethyl aminoethyl methacrylate (DMAEMA) (1:3) , **(S-4IPN)** and **(S-4IPNC)** with a ratio of acrylic acid (AA) to dimethyl aminoethyl methacrylate (DMAEMA) (1:4) as ratio of castor oil to carboxymethyl cellulose (CMC) (1:2) in case of S- 2IPNC,S-3IPNC and S-4IPNC.

4. Factors affecting on swelling properties

*4.1. Effect of temperature:*In order to investigate the effect of temperature on swelling behavior, the other parameters are kept constant (pH 7 and 0 M salt concentration). The maximum water absorption (Qmax) of the prepared hydrogels, namely, S-2IPN, S-3IPN, S-4IPN, S-2IPNC, S-3IPNC and S-4IPNC were measured as a function of temperature within the range of 25-45 ºC, Fig. (7a). The maximum water absorbance was achieved nearly after 2hrs. The temperature / Qmax curves show that the investigated hydrogels respond effectively to the temperature and release the absorbed water when approaching their LCST, which proves their usability under different environmental conditions. The data revealed that the order of water absorption is as follows: S-4IPNC, S-3IPNC, S-2IPNC, S-4IPN, S-3IPN and S-2IPN respectively as shown in table (3). It can be seen that- beyond a certain temperature- the rate of swelling decreases sharply (above the LCST the network becomes more compact and the interpenetration of the water into the network comes to be very difficult) Also, it is clear that the swelling is more efficient upon increasing the weight ratio of DMAEMA to the acrylic acid i.e. (S-4IPNC). This improvement in the swelling is due to that the presence of carboxylic groups which increase electrostatic repulsion between the carboxylate ions-COO-) [51] The swelling behavior of the hydrogels can be explained by the following assumption: the bonding of Carboxymethylcellulose (CMC) to polyacrylamide (PAAm), a hydrophilic material, promotes these materials to change its hydrophilic nature when the temperature approaches the LCST as shrinkage occurs and swelling decreases due to phase separation. According to the temperature where hydrogel releases it is half of the absorbed water (LCST) occurs at 35ºC, as LCST of PDMAEMA showed in the range of 32–55 0C [52, 53].

Table (3): Swelling ratio percentage of prepared hydrogels

Sample Code	Qmax(g/g)	SR%	No. of cycles	Conditions
S-4IPNC	208.348 $g.g^{-1}$	20734.8%	6	25ºC, 0M, pH7
S-3IPNC	191.21$g.g^{-1}$	19021%	6	25ºC, 0M, pH7
S-2IPNC	175.82 $g.g^{-1}$	17482%	6	25ºC, 0M, pH7
S-4IPN	159.35 $g.g^{-1}$	15835%	5	25ºC, 0M, pH7
S-3IPN	145.21 $g.g^{-1}$	14421%	5	25ºC, 0M, pH7
S-2IPN	123.82 $g.g^{-1}$	12282%	5	25ºC, 0M, pH7

*4.2. Effect of salt:*The maximum water absorption (Qmax) was monitored for the investigated hydrogels at different NaCl saline solutions (0.2 M, 0.6M and 1M) keeping other variables constant, i.e., 25 ºC and pH 7. It is observed from fig. (7b) that prepared hydrogels are salt responsive, i.e., the Q max for all the investigated hydrogels decreases with increasing salinity of the absorbed water. For instant, when salinity increases from 0.2 M to 1 M i.e., 5 folds. The Q max of S-4IPNC has reduced from (192.8g/g) to (178.2 g/g). While Qmax of S-2IPN was (136.7 g/g) at 0.2M. The swelling behavior of hydrogels in a salt solution can be explained by the interaction between fixed ions on the hydrogel and mobile ions, which are affected by the salt concentration and the osmotic pressure. As the fixed ions on hydrogel attract mobile charges in the environmental solution that leads to an imbalance of ions concentration between the hydrogel and outer solution, and finally, the deformation of hydrogel occurs [54, 55]. At a high salt concentration of NaCl solution, Qmax decreases due to decreasing in Donnan osmotic pressure as the competitive effect of the ions of the salt on the active sites with the water molecules occurs. The difference between the concentration of Na^+ and Cl^- ions in the external and swelling medium decreases, which subsequently leads to decrease hydrogel swelling [56].

4.3. Effect of pH:

The effect of pH on the swelling properties of S-2IPN, S-3IPN, S-4IPN, S-2IPNC, S-3IPNC and S-4IPNC is shown in Fig. (7C) at pH values 5, 7 and 9. As the prepared hydrogels are composed of interpenetrating polymer networks based on carboxyl

methylcellulose and two crosslinked polymers, one of them is thermoresponsive, and the other is pH-responsive to achieve the dual function. An increase in swelling ratios from pH (5-7) was observed and then a sharp decrease in water uptake was observed from pH (7-9). In the acidic medium (At pH > 4), the osmotic pressure inside the hydrogel increases lead to higher swelling because of the dissociation of carboxyl groups that exist in hydrogels. While at pH > 7, i.e., basic medium, the concentration of basic cations in the outer solution increases and a further amount of mobile ions increases which leads to decrease osmotic pressure and eventually reducing water absorption [57].

For an instant, when pH increases from 5 to 7. The Qmax of S-4IPNC has increased from (191.5 g/g) to (208 g/g) then back to reduced when pH reaches 9. While Qmax of S-2IPN was (123.8 g/g) at neutral medium.

The incorporation of a long chain of castor oil within the network affords the network structure with flexibility and increases the size of the pores available for water capturing. Therefore, the samples with castor oil incorporated inside their 3D structure showed higher swelling in comparison to their counterparts. Up to our knowledge, it is the first time to include castor oil in such formulations; therefore, there are no data available to compare our data with.

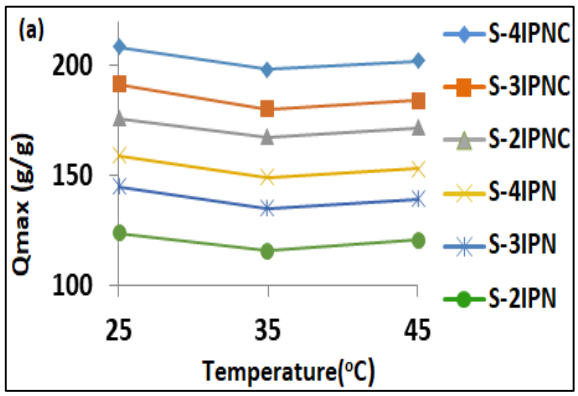

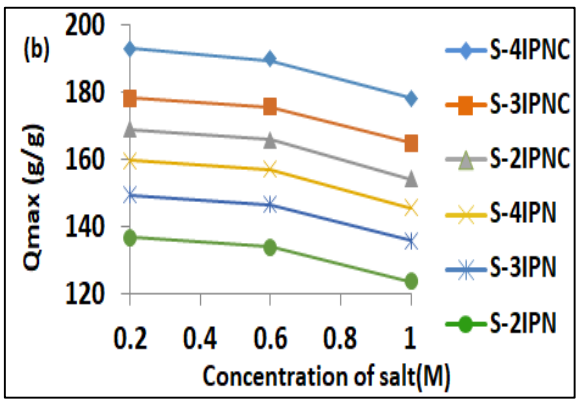

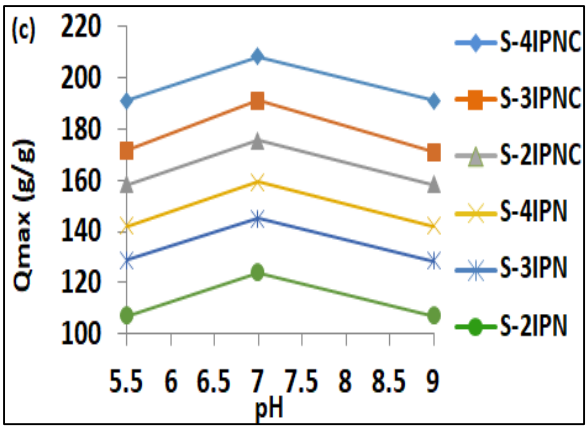

Fig. (7) : Water absorption for semi-interpenetrating polymer networks **(S-4IPN) ,(S-3IPN) , (S-2IPN)** with a ratio of acrylic acid (AA) to dimethyl aminoethyl methacrylate (DMAEMA) (1:4) , (1:3) and (1:2) respectively and semi-interpenetrating polymer network (S-**4IPNC) ,(S-3IPNC) , (S-2IPNC)** with a ratio of acrylic acid (AA) to dimethyl aminoethyl methacrylate (DMAEMA) (1:4) , (1:3) and (1:2) respectively and ratio of castor oil to carboxymethyl cellulose (CMC) (1:2) under **a)** effect of temperature **(b)** effect of salinity and **(c)** effect of pH.

5. Re-swelling capability of interpenetrating network hydrogel

Swelling-deswelling capability is one of the most important parameters judging the workability of hydrogels in agricultural areas[58]. The water absorbency of the interpenetrating network hydrogel structures in distilled water as a function of the number of reswelling times is shown in Fig. 8. The swelling capacity of hydrogel samples gradually decreases with increasing the number of reswelling cycles as S-IPNC hydrogels show 6 cycles as Qmax starts to increase gradually from 208.348 g/g (20734.8%) in 1st cycle then decay in 6th cycle to be 95.138g/g (9413.8%). While S-IPN hydrogels show 5 cycles as Qmax start to increase gradually from 123.82 g/g (12282%) in 1st cycle then decay in 5th cycle to be 32.315 g/g (3131.5%) as shown in table (3). This is probably due to the breakage of physical crosslinking points of S-IPN networks in the repeating process of swelling-reswelling, causing severe damage to polymeric network structures [59]. Therefore, the ability of the hydrogel for holding water is gently diminished and the equilibrium water absorbency is decreased consecutively. This result displays that the S-IPN hydrogel has maintained at a certain degree of swelling capability after reused for several cycles. Therefore, the obtained interpenetrating network hydrogels could be used as reusable and recyclable materials in many fields. Moreover, it is shown that increasing concentration of the hydrophilic monomer DMAEMA into interpenetrating network hydrogel significantly enhances the reswelling capability of the network. Finally, table (3) show that S-4IPNC was the highest water absorbance and S-2IPN was the lowest one.

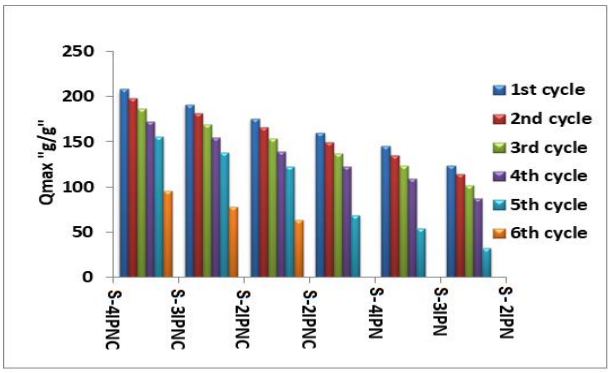

Fig. (8): cycles of swelling-deswelling for semi-interpenetrating polymer networks **(S-4IPNC) ,(S-3IPNC) ,(S-2IPNC)** with a ratio of acrylic acid (AA) to dimethyl aminoethyl methacrylate (DMAEMA) (1:4) , (1:3) and (1:2) respectively and ratio of castor oil to carboxymethyl cellulose (CMC) (1:2) and **(S-4IPN) ,(S-3IPN) , (S-2IPN)** with a ratio of acrylic acid (AA) to dimethyl aminoethyl methacrylate (DMAEMA) (1:4) , (1:3) and (1:2) respectively .

6. Mechanism of water release from swelling hydrogels

The hydrophilic groups present in the polymer e.g. (acrylamide, carboxylic acid, etc.) are in charge of water absorption in hydrogels. These hydrophilic groups are attached to the chain of the polymer. Upon interaction between 3D polymer network structure and water molecules, several negative COO- groups appeared and repel each other and finally the chain opened up, also numerous hydrogen bondings occur between –COO- groups, –NH groups and water molecules causing more water absorption and more swelling. These bondings are disturbed under the effect of the environmental changes such as temperature, salinity and pH, that lead to a release of some water molecule and shrinkage of polymer network consequently happens.

At 25 °C, for S-4IPNC, S-3IPNC, the polymer network formed hydrogen bonds with the water molecules, developing a hydration shell around the hydrophilic group which enhanced water uptake capacity to high absorbency (208 g/g) and (191 g/g) respectively while S-2IPN show the lowest Qmax (123.8 g/g). However, with increasing temperature, the absorbency steadily decreased due to the elasticity of the cross-linked polymer network leading to the release of absorbed water. The collapse of the hydration shell at high temperature may be responsible for the decrease in absorbency capacity. The polymer 3D network structure collapses due to destabilization of the polymer network structure, under different factors as Temperature, pH and salt medium, leading to synerisis[60]. In a salty medium, for S-4IPNC, S-3IPNC the maximum water absorbance was observed at low sodium salt concentration (0.2M) to reach (192.8g/g) and (178 g/g) respectively, then it decreases subsequently in high NaCl concentration while S-2IPN show the lowest Qmax (136.7g/g). This Phenomenological occurrence can be attributed to the effect of the additional cations which cause a decrease in anion–anion electrostatic repulsion, resulting in a decrease in the osmotic pressure difference between the polymer networks and the external solution. The difference in mobile ion concentration between the polymer networks and liquid phases decreases resulting in a decrease in absorbency capacity [60, 61]. Regarding pH, at neutral medium, S-4IPNC and S-3IPNC show the highest maximum water absorbance (208 g/g) and (191 g/g) respectively while S-2IPN show the lowest Q_{max} (123.8 g/g) as shown in table (3). While in acidic conditions below 6 or basic conditions of above 8 generally lowered the swelling ratio with a favourable ratio in the range of 6-8 being identified. The results show that high temperature above 40°C, high salt concentration(1M) and basic medium at pH=9 usually result in a collapse of the 3-D network structure. The phenomena of water absorption and desorption are shown in Fig. (9).

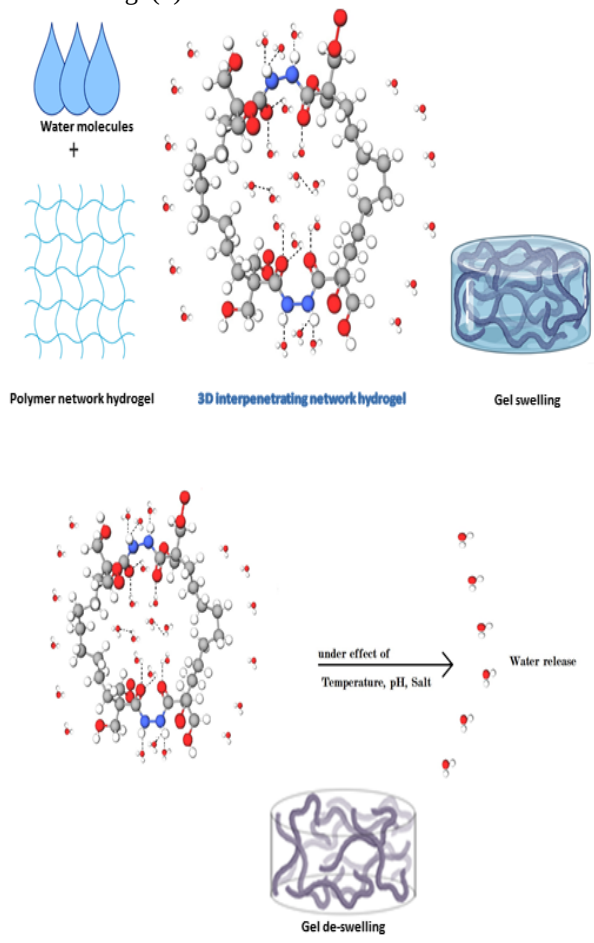

Fig. (9): Mechanism of absorption-desorption process.

7. Conclusion

In this study, AA-PDMAEAM/CMC semi-interpenetrating polymer networks were synthesized by crosslinking between AA and DMAEMA monomers in the presence of N, N′-methylene bisacrylamide (MBA) as a crosslinking agent using CMC with and without castor oil. S-3IPNC was taken as a representative sample which shows a better surface morphology and topography approved by SEM and AFM, respectively, and thermogravimetric analysis shows that a higher concentration of castor oil improved the thermal resistance as the hydrogels, which have castor oil in their backbone, are more stable than their counterparts. Swelling measurements of S-IPN and S-IPNC hydrogels were carried out under various environmental conditions (i.e., temperature, salinity and pH). It is concluded that high temperature above 40°C, high salt concentration (1M) and basic medium at pH=9 usually results in a collapse of the 3-D network structure of (S-IPN/S-IPNC) hydrogels while at (25ºC, 0 M , pH 7), S-4IPNC show highest swelling ratio (208g/g) while S-2IPN was the lowest one (123.8g/g).TGA and AFM characterization has assured the role of the castor oil to acquire samples stiffness and rigid texture. The addition of castor oil indicates the potential green applications of AA-PDMAEMA/CMC semi-interpenetrating polymer network (S-IPNC) for different environmental areas.
In comparison with different vegetable oils, castor oil can be stored for a long time and stay usable. Castor oil, as a renewable source, can be utilized as a starting material in the synthesis of bio-based polymers and can be used for upcoming applications.

8. Conflicts of interest

"There are no conflicts to declare".

9.Acknowledgments

The authors acknowledge the Egyptian petroleum research institute (EPRI) for supporting this work.

10. References

[1] M. Abdel-Raouf, A. Abdul-Raheim, Removal of heavy metals from industrial waste water by biomass-based materials: a review, Journal of Pollution Effects & Control 5(1) (2017) 1-13.

[2] A.-R.M. Abdul-Raheim, M. El-Saeed Shimaa, K. Farag Reem, E.J.A.M.L. Abdel-Raouf Manar, Low cost biosorbents based on modified starch iron oxide nanocomposites for selective removal of some heavy metals from aqueous solutions, 7(5) (2016) 402-409. https://doi.org/10.5185/amlett.2016.6061

[3] R.K. Farag, S.M. EL-Saeed, M.E.J.D. Abdel-Raouf, W. Treatment, Synthesis and investigation of hydrogel nanoparticles based on natural polymer for removal of lead and copper (II) ions, 57(34) (2016) 16150-16160.https://doi.org/10.1080/19443994.2015.1077744.

[4] S.M. Elsaeed, R.K. Farag, N.S. Maysour, Synthesis and characterization of pH- sensitive crosslinked (NIPA- co- AAC) nanohydrogels copolymer, Journal of Applied Polymer Science 124(3) (2012) 1947-1955.

[5] E.M. Ahmed, Hydrogel: Preparation, characterization, and applications: A review Journal of advanced research 6(2) (2015) 105-121. https://doi.org/10.1016/j.jare.2013.07.006.

[6] M.I.H. Mondal, M.O. Haque, Cellulosic Hydrogels: A Greener Solution of Sustainability, Cellulose-Based Superabsorbent Hydrogels (2019) 3-35.

[7] M.E. Abdel-Raouf, S.M. El-Saeed, E.G. Zaki, A.M. Al-Sabagh, Green chemistry approach for preparation of hydrogels for agriculture applications through modification of natural polymers and investigating their swelling properties, Egyptian journal of petroleum 27(4) (2018) 1345-1355.

[8] T. Li, F. Huang, D. Diaz-Dussan, J. Zhao, S. Srinivas, R. Narain, W. Tian, X. Hao, Preparation and Characterization of Thermo-Responsive PEG Based Injectable Hydrogels and their Application for 3D Cell Culture, Biomacromolecules (2020).

[9] W. Tanan, J. Panichpakdee, S. Saengsuwan, Novel biodegradable hydrogel based on natural polymers: Synthesis, characterization, swelling/reswelling and biodegradability, European Polymer Journal 112 (2019) 678-687.

[10] A. Roy, P.P. Maity, A. Bose, S. Dhara, S.J.M.c.f. Pal, β-Cyclodextrin based pH and thermo-responsive biopolymeric hydrogel as a dual drug carrier, 3(3) (2019) 385-393. https://doi.org/10.1039/C8QM00452H.

[11] E. Motamedi, B. Motesharezedeh, A. Shirinfekr, S.M. Samar, Synthesis and swelling behavior of environmentally friendly starch-based superabsorbent hydrogels reinforced with natural char nano/micro particles, Journal of Environmental Chemical Engineering 8(1) (2020) 103583. https://doi.org/10.1016/j.jece.2019.103583.

[12] Ö.B. Üzüm, İ. Bayraktar, S. Kundakcı, E. Karadağ, Swelling behaviors of novel magnetic semi-IPN hydrogels and their application for Janus Green B removal, Polymer Bulletin 77(2)

(2020) 847-867. https://doi.org/10.1007/s00289-019-02781-4.
[13] G.R. Bardajee, S.S. Hosseini, C.J.N.J.o.C. Vancaeyzeele, Graphene oxide nanocomposite hydrogel based on poly (acrylic acid) grafted onto salep: an adsorbent for the removal of noxious dyes from water, 43(8) (2019) 3572-3582. https://doi.org/10.1039/C8NJ05800H.
[14] Z. Zhao, H.J. Qi, D. Fang, A finite deformation theory of desolvation and swelling in partially photo-cross-linked polymer networks for 3D/4D printing applications, Soft matter 15(5) (2019) 1005-1016. https://doi.org/10.1039/C8SM02427H.
[15] H. Shoukat, K. Buksh, S. Noreen, F. Pervaiz, I.J.T.D. Maqbool, Hydrogels as potential drug-delivery systems: network design and applications, (0) (2021).
[16] K. Joshy, S. Snigdha, S. Thomas, T.J.N.H. Li, An Overview of the Recent Developments in Hydrogels, (2021) 231-246.
[17] Y. Zhang, Z. Li, J. Guan, Y. Mao, P.J.A.A. Zhou, Hydrogel: A potential therapeutic material for bone tissue engineering, 11(1) (2021) 010701.
[18] G. Janarthanan, I.J.J.o.M.S. Noh, Technology, Recent trends in metal ion based hydrogel biomaterials for tissue engineering and other biomedical applications, 63 (2021) 35-53.
[19] L. Tang, S. Wu, J. Qu, L. Gong, J.J.M. Tang, A Review of Conductive Hydrogel Used in Flexible Strain Sensor, 13(18) (2020) 3947.
[20] A. Zhang, F. Wang, L. Chen, X. Wei, M. Xue, F. Yang, S.J.C.C.L. Jiang, 3D printing hydrogels for actuators: A review, (2021).
[21] Z. Wu, X. Yang, J.J.A.A.M. Wu, Interfaces, Conductive hydrogel-and organohydrogel-based stretchable sensors, 13(2) (2021) 2128-2144.
[22] J.M. Passantino, K.D. Wolfe, K.T. Simon, D.E. Cliffel, G.K.J.A.A.B.M. Jennings, Photosystem I Enhances the Efficiency of a Natural, Gel-Based Dye-Sensitized Solar Cell, 3(7) (2020) 4465-4473.
[23] S. Galliano, F. Bella, M. Bonomo, G. Viscardi, C. Gerbaldi, G. Boschloo, C.J.N. Barolo, Hydrogel electrolytes based on xanthan gum: Green route towards stable dye-sensitized solar cells, 10(8) (2020) 1585.
[24] F. Bella, A. Chiappone, J. Nair, G. Meligrana, C.J.C.E.T. Gerbaldi, Effect of different green cellulosic matrices on the performance of polymeric dye-sensitized solar cells, 41 (2014) 211-216.
[25] N. Mariotti, M. Bonomo, L. Fagiolari, N. Barbero, C. Gerbaldi, F. Bella, C.J.G.C. Barolo, Recent advances in eco-friendly and cost-effective materials towards sustainable dye-sensitized solar cells, 22(21) (2020) 7168-7218.
[26] L. Fagiolari, M. Bonomo, A. Cognetti, G. Meligrana, C. Gerbaldi, C. Barolo, F. Bella, Photoanodes for Aqueous Solar Cells: Exploring Additives and Formulations Starting from a Commercial TiO2 Paste, (2020).
[27] V. Kumar, V. Rehani, B.S. Kaith, Synthesis of a biodegradable interpenetrating polymer network of Av-cl-poly (AA-ipn-AAm) for malachite green dye removal: kinetics and thermodynamic studies, RSC advances 8(73) (2018) 41920-41937.
[28] Y.-J. Kim, Y.T. Matsunaga, Thermo-responsive polymers and their application as smart biomaterials, Journal of Materials Chemistry B 5(23) (2017) 4307-4321.
[29] A. Teotia, H. Sami, A. Kumar, Thermo-responsive polymers: structure and design of smart materials, Switchable and responsive surfaces and materials for biomedical applications, Elsevier2015, pp. 3-43.
[30] Z. Lin, Y. Yang, A. Zhang, Polymer-engineered nanostructures for advanced energy applications, Springer2017.
[31] P. Ramakrishna, K.M. Rao, K. Sekharnath, P. Kumarbabu, S. Veeraprathap, K.C. Rao, M.J.J.o.A.P.S. Subha, Synthesis and characterization of Interpenetrating polymer network microspheres of acryl amide grafted Carboxymethylcellulose and Sodium alginate for controlled release of Triprolidine hydrochloride monohydrate, 3(3) (2013) 11. https://doi.org/10.7324/JAPS.2013.30320
[32] S.D. Miao, Y.Y. Liu, P. Wang, S.P. Zhang, Castor oil and microcrystalline cellulose based polymer composites with high tensile strength, Advanced Materials Research, Trans Tech Publ, 2012, pp. 1531-1535.
[33] X. Huang, H. Liu, S. Shang, Z. Cai, J. Song, Z.J.F.o.A.S. Song, Engineering, Synthesis and characterization of castor oil-based polymeric surfactants, 3(1) (2016) 46-54.
[34] V.J. Dave, H.S.J.J.o.S.C.S. Patel, Synthesis and characterization of interpenetrating polymer networks from transesterified castor oil based polyurethane and polystyrene, 21(1) (2017) 18-24.
[35] E.B. Mubofu, Castor oil as a potential renewable resource for the production of functional materials, Sustainable Chemical Processes 4(1) (2016) 11.
[36] K.P. Ramaiah, K. Mishra, A. Atkar, S.J.C.E.J. Sridhar, Pervaporation Separation of Chlorinated

Environmental Pollutants from Aqueous Solutions by Castor Oil based Composite Interpenetrating Network Membranes, (2020) 124050.

[37] S. Chen, Q. Wang, T.J.M. Wang, Design, Damping, thermal, and mechanical properties of carbon nanotubes modified castor oil-based polyurethane/epoxy interpenetrating polymer network composites, 38 (2012) 47-52.

[38] A. Shirke, B. Dholakiya, K. Kuperkar, Novel applications of castor oil based polyurethanes: a short review, Polymer Science Series B 57(4) (2015) 292-297. https://doi.org/10.1134/S1560090415040132.

[39] M.J.J.o.m.s. Begum, Synthesis and characterization of polyurethane/polybutyl methacrylate interpenetrating polymer networks, 39(14) (2004) 4615-4623.

[40] E. Nekhavhambe, H.E. Mukaya, D.B.J.J.o.A.M. Nkazi, Processing, Development of castor oil–based polymers: A review, 1(4) (2019) e10030.

[41] D.J.I.J.o.P.S. Braun, Origins and development of initiation of free radical polymerization processes, 2009 (2009).

[42] Q. Li, Z. Ma, Q. Yue, B. Gao, W. Li, X. Xu, Synthesis, characterization and swelling behavior of superabsorbent wheat straw graft copolymers, Bioresource technology 118 (2012) 204-209. https://doi.org/10.1016/j.biortech.2012.03.028.

[43] Y. Bao, J. Ma, N. Li, Synthesis and swelling behaviors of sodium carboxymethyl cellulose-g-poly (AA-co-AM-co-AMPS)/MMT superabsorbent hydrogel, Carbohydrate Polymers 84(1) (2011) 76-82. https://doi.org/10.1016/j.carbpol.2010.10.061.

[44] A. Pourjavadi, P.E. Jahromi, F. Seidi, H. Salimi, Synthesis and swelling behavior of acrylatedstarch-g-poly (acrylic acid) and acrylatedstarch-g-poly (acrylamide) hydrogels, Carbohydrate Polymers 79(4) (2010) 933-940. https://doi.org/10.1016/j.carbpol.2009.10.021.

[45] Y. Katsumoto, T. Tanaka, Y. Ozaki, Molecular Interpretation for the Solvation of Poly (acrylamide) s. I. Solvent-Dependent Changes in the CO Stretching Band Region of Poly (N, N-dialkylacrylamide) s, The Journal of Physical Chemistry B 109(44) (2005) 20690-20696. https://doi.org/10.1021/jp052263r.

[46] D. Roy, J.T. Guthrie, S. Perrier, Synthesis of natural–synthetic hybrid materials from cellulose via the RAFT process, Soft Matter 4(1) (2008) 145-155. https://doi.org/10.1039/b711248n.

[47] Y. Katsumoto, T. Tanaka, Y. Ozaki, S.J.V.S. Hosoi, Effects of dipole interaction and solvation on the CO stretching band of N, N-dimethylacetamide in nonpolar solutions: Infrared, isotropic and anisotropic Raman measurements, 51(1) (2009) 119-124.

[48] M. Trouilh, D. Hourdet, A. Marcellan, P.J.R.d.M. Colomban, C. Avancés, Analyse Raman in situ de la déformation d'un hydrogel nanocomposite, 24(1) (2014) 67.

[49] H. Edwards, A. Johnson, E. Lawson, A Raman spectroscopic study of N, N-dimethylacrylamide, Spectrochimica Acta Part A: Molecular Spectroscopy 50(2) (1994) 255-261. https://doi.org/10.1016/0584-8539(94)80054-5.

[50] E. Valles, D. Durando, I. Katime, E. Mendizabal, J. Puig, Equilibrium swelling and mechanical properties of hydrogels of acrylamide and itaconic acid or its esters, Polymer bulletin 44(1) (2000) 109-114. https://doi.org/10.1007/s002890050580.

[51] N. Seddiki, D.J.B.o.t.C.S.o.E. Aliouche, Synthesis, rheological behavior and swelling properties of copolymer hydrogels based on poly (N-isopropylacrylamide) with hydrophilic monomers, 27(3) (2013) 447-457.

[52] Z. Alinejad, F. Khakzad, A.R. Mahdavian, Efficient approach to in-situ preparation of anisotropic and assemblable gold nanoparticles mediated by stimuli-responsive PDMAEMA, European Polymer Journal 104 (2018) 106-114. https://doi.org/10.1016/j.eurpolymj.2018.05.006.

[53] T. Manouras, E. Koufakis, S.H. Anastasiadis, M. Vamvakaki, A facile route towards PDMAEMA homopolymer amphiphiles, Soft matter 13(20) (2017) 3777-3782. https://doi.org/10.1039/c7sm00365j.

[54] C. Chang, M. He, J. Zhou, L. Zhang, Swelling behaviors of pH-and salt-responsive cellulose-based hydrogels, Macromolecules 44(6) (2011) 1642-1648. https://doi.org/10.1021/ma102801f.

[55] K. Goh, H. Li, K. Lam, Modeling the urea-actuated osmotic pressure response of urease-loaded hydrogel for osmotic urea biosensor, Sensors and Actuators B: Chemical 268 (2018) 465-474. https://doi.org/10.1016/j.snb.2018.04.137.

[56] K.M. Salleh, S. Zakaria, M.S. Sajab, S. Gan, C.H. Chia, S.N.S. Jaafar, U.A. Amran, Chemically crosslinked hydrogel and its driving force towards superabsorbent behaviour, International journal of biological macromolecules 118 (2018) 1422-1430. https://doi.org/10.1016/j.ijbiomac.2018.06.159.

[57]S. Nesrinne, A. Djamel, Synthesis, characterization and rheological behavior of pH sensitive poly (acrylamide-co-acrylic acid) hydrogels, Arabian Journal of Chemistry 10(4) (2017) 539-547. https://doi.org/10.1016/j.arabjc.2013.11.027.

[58] Q. Li, Z. Ma, Q. Yue, B. Gao, W. Li, X.J.B.t. Xu, Synthesis, characterization and swelling behavior of superabsorbent wheat straw graft copolymers, 118 (2012) 204-209.
[59] X. Xu, B. Bai, C. Ding, H. Wang, Y.J.I. Suo, E.C. Research, Synthesis and properties of an ecofriendly superabsorbent composite by grafting the poly (acrylic acid) onto the surface of dopamine-coated sea buckthorn branches, 54(13) (2015) 3268-3278.
[60]R. Mahon, Y. Balogun, G. Oluyemi, J.J.S.A.S. Njuguna, Swelling performance of sodium polyacrylate and poly (acrylamide-co-acrylic acid) potassium salt, 2(1) (2020) 1-15.
[61] X.-F. Sun, Y. Hao, Y. Cao, Q.J.I.j.o.b.m. Zeng, Superadsorbent hydrogel based on lignin and montmorillonite for Cu (II) ions removal from aqueous solution, 127 (2019) 511-519.

تحضيروتوصيف عائلة جديدة من شبكات الهيدروجيل المتداخلة البينية بواسطة طريقة خضراء.

آلاء ابراهيم السيد عبد العزيز [1] , شيماء محمد السعيد[1] , السيد جمال ذكى[1], محمد محمود محمد أبو على[2] ,منارالسيدعبدالرءوف[1] , أحمد محمد الصباغ[1]

[1] معهد بحوث البترول, 1 شارع أحمد الزمر- حى الزهور- مدينة نصر-القاهرة – مصر.
[2] قسم الكيمياء -- كلية العلوم- جامعة عين شمس-القاهرة- مصر.

في هذا البحث يتم تحضير شبكات البوليمرات المتداخلة فى وجود و غياب زيت الخروع (S-2IPNC, S-3IPNC, S-4IPNC, S-2IPN, S-3IPN and S-4IPN)عن طريق عملية بلمرة الشقوق الحرة فى وجود كلا من حمض الأكريليك كمونومر مستجيب للأس الهيدروجيني وثنائي ميثيل إيثيل ميثاكريلات كمونومر مستجيب للحرارة وكربوكسى ميثيل السليلوز كمشتق سليلوزى وكذلك البوتاسيوم بيرسلفات والميثيلين بيساكريلاميد. يتم دمج زيت الخروع كمادة كيميائية خضراء بنسبة (1: 2) إلى الكربوسى ميثيل سليلوز. تم تحضير شبكات البوليمر المتداخلة وتوصيفها بواسطة تقنيات مختلفة مثل الأشعه تحت الحمراء وأشعة الرامان الطيفي لدراسة تركيبها الكيميائى وكذلك تحليل الثبات الحرارى والميكروسكوب الالكترونى الماسح والأشعة السينية وميكروسكوب القوة الذرية لدراسة كلا من التحليل الحراري الوزني ، وتضاريس السطح ، والتبلور، وطبوغرافيا السطح ، على التوالي. وأثبت الدراسات ان إضافة زيت الخروع يعززمن نسيج وثبات الهيدروجلات. وتشير نتائج الدراسات الى أن S-IPNC يظهر قدرة امتصاص أعلى من S-IPN عند تركيزات منخفضة من كلوريد الصوديوم وفى نطاق الأس الهيدروجيني (5-7) وذلك بسبب زيادة الضغط الأسموزى. لذلك ، يمكن استخدام زيت الخروع كمادة خضراء في شبكات البوليمرالمتداخلة وتطبيقها لتوفيرالمياه وبذلك تمتلك الهيدروجيلات البينية إمكانية كبيرة لتخزين المياه لاستخدامها في المجال الزراعي.